Effect of joint line remnant on fatigue lifetime of friction stir welded Al–Cu–Li alloy

T. Le Jolu*, T. F. Morgeneyer and A. F. Gourgues-Lorenzon

The effect of joint line remnant (JLR) on the fatigue lifetime of friction stir welds of a 2198 Al alloy in T851 condition has been assessed experimentally. The base material, sound welds (welded in one sheet) and welds with JLR (produced via welding of two sheets with a natural oxide layer) have been investigated. A strong decrease in microhardness is found for the weak weld zone that is consistent with the reduction in tensile properties compared to the base material: 45% in yield strength and 22% in ultimate tensile strength. The fatigue strengths of sound and JLR bearing welds at 100 000 cycles (R=0·1) are reduced by 10 and 15% respectively compared to the base material. Only for one-third of the JLR bearing specimens, the fatigue crack initiated in regions close to the JLR and this without reduction in fatigue lifetime.

Keywords: Friction stir welding, Fatigue, Joint line remnant, Al–Cu–Li

Introduction

The latest generation of Al–Cu–Li alloys is considered as candidate alloys for future aerospace applications thanks to their beneficial density to strength ratio, good mechanical properties and corrosion resistance compared to other damage tolerant alloys, leading to a growing interest in these alloys.[1–3] Additionally, the requirement of weight and cost savings in the transport industry leads to increasing interest in joining processes. Among the various existing techniques, friction stir welding (FSW) is now emerging as a viable solid state process for joining aluminium alloys used in marine, automotive or aerospace industry. The advantages of using this process are mainly the possibilities to weld alloys traditionally considered as unweldable, the absence of defects such as porosities or cracks and the low distortion and residual stresses resulting from melting and solidification.[4–6]

In recent studies, particular attention has been drawn to a FSW defect in Al alloys, which results from the natural oxide layer on butt surfaces, which is mixed during the welding process. It consists in a discontinuous line of oxide particles which crosses the weld thickness. The designation for this defect and its characterisation does not seem to be established yet. In the literature the defect is referred to as 'joint line remnant' (JLR), 'lazy S', 'zigzag curve', 'zigzag line'.[7–10] When the defect is linked to the weld root it is also referred to as 'root flaw' or 'kissing bond' or 'weak bond'.[7,11,12] Welding conditions (e.g. insufficient tool plunge depth) may lead to this defect at the weld root.[12] In the present study, the 'JLR' and 'kissing bond' will respectively be used to distinguish defects that respectively do and do not meet the weld root. It seems difficult to avoid the JLR even using stable and optimised welding conditions.[7,11] The bonding between the welded parts is often assessed via bending tests revealing that the kissing bond is the most detrimental defect and may lead to bending fracture initiation.[7,12,13]

The influence of the JLR or kissing bond defect on the fatigue properties has been studied for various Al alloys.[7,12–15] Some authors report a non-systematic fatigue crack initiation on a JLR[15] or on a kissing bond-like defect,[7,12–14] but for others[10] no effect of the JLR is found. In all studies a reduction in fatigue lifetime of the FSW assembly with respect to the base material is found. In several studies a comparison with literature results on supposedly sound welds is made, highlighting a strong reduction in fatigue strength (up to 50%).[14] To summarise, it seems difficult, at present, to conclude on the reduction in fatigue lifetime due to the JLR or kissing bond defect compared to the welds without these defects. Cantin *et al.*[16] have identified that for lap joints in 5083-O the tensile and fatigue properties can be substantially improved by using friction skew stir welding (trade name). In this technique the axis of the tool has a slight inclination with respect to that of the machine spindle. As a result a wider weld region, a more effectively mixed initial oxide layer and smaller voids around the JLR are obtained. However, in this study and for the potential aerospace application butt welds are to be studied for a different alloy type and it is anticipated that the mechanical properties of friction skew stir welds compared to conventional FSW welds will hardly be superior.

In the present work, a novel strategy to assess the effect of the JLR on the fatigue behaviour of 2198-T8 friction stir welds is suggested via testing sound welds (welded in one sheet) and welds with a JLR (obtained by joining two sheets with their natural oxide layer) while keeping reproducible welding and testing conditions.

MINES ParisTech, Centre des Matériaux, CNRS UMR 7633, BP 87, 91003 Evry Cedex, France

*Corresponding author, email thomas.le_jolu@mines-paristech.fr

Published by Maney on behalf of the Institute
Received 4 May 2010; accepted 9 July 2010
DOI 10.1179/136217110X12813393169453

Experimental

The material used in this study is a 2198-T851 Al–Cu–Li alloy sheet with a thickness of 3·1 mm. The material has been produced by ALCAN (Montreal, Canada). The chemical composition of this alloy is Al–3·20Cu–0·98Li–0·31Ag–0·31Mg–0·11Zr–0·04Fe–0·03Si (wt-%). In this study the rolling direction will be referred to as L, the long transverse direction as T and the short transverse direction as S. Blanks cut from the sheet were joined by FSW by ONERA (Paris, France) along the L direction using the welding parameters and tool geometry reported in Table 1. Two types of welds were produced: welds without JLR (referred to as sound welds here) and welds containing a JLR defect. The sound welds were produced via welding in one sheet whereas for the welds with JLR two sheets that were naturally oxidised before welding were joined. All welds were tested under the as welded condition. The grain structures of the base material and of the welds, and in particular the JLR defects were observed using polarised light optical microscopy after etching with a 3% HBF_4 aqueous solution. The local mechanical properties of welds were assessed by HV0·1 Vickers microhardness measurements on T–S cross-weld polished sections. These measurements were performed along lines through the weld and parallel to the T direction. These lines were chosen at various locations in the sheet thickness (0·5, 1·5 and 2·5 mm from the sheet edge). The tensile tests were carried out at room temperature using a 250 kN servohydraulic testing machine under displacement control with an initial strain rate of 2×10^{-4} s^{-1}. Tests were performed along L and T directions for the base material and along the T direction for the welded material, i.e. across the weld. For the base material three tests were performed for each testing direction and results were very reproducible. The geometry of tensile specimens is shown in Fig. 1. The weld line is located at the centre of the specimen and the initial gauge length of the longitudinal extensometer was 25 mm, i.e. about two times larger than the weld width. Fatigue specimens were tested at room temperature along both L and T directions for the base material and along the T (i.e. cross-weld) direction for the welded material. The fatigue tests were carried out using a servohydraulic testing machine with a load capacity of 250 kN. A sinusoidal load–time function was used, applying a stress ratio R of 0·1 and using a frequency of 20 Hz. The chosen geometries of fatigue specimens for the base material and for the welded material are shown in Figs. 2 and 3 respectively, according to ASTM E466-07 testing standard.[17] The base material fatigue specimen has continuous radius between ends to avoid crack initiation from the fillets. For the welded material, the specimen shows tangentially blending fillets, so that all areas of the welded joint are exposed to the same engineering stress level. Before testing, specimens were ground at the corners to limit the stress concentrations and on the surfaces with 600 and 1200 SiC paper parallel to the loading direction to avoid fatigue crack initiation from surface tool rotation marks. After the tests, fracture surfaces were examined using an LEO 1450 VP scanning electron microscope (SEM).

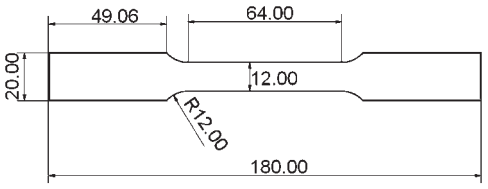

1 Specimen geometry for tensile testing

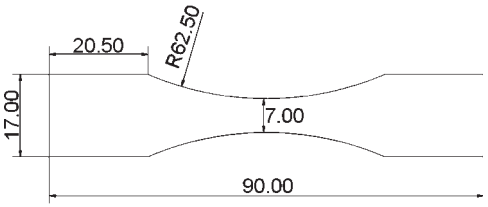

2 Base material specimen geometry for fatigue testing

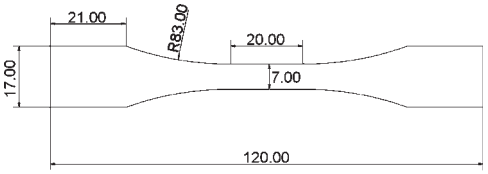

3 Cross-weld specimen geometry for fatigue testing

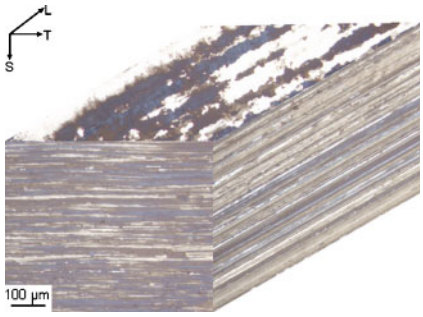

4 Light optical micrographs of grain structure of base material

5 Light optical micrograph of sound weld

Results

Microstructure

Optical micrographs of the grain structure of the base material showed pancake shaped grains lying in the L–T plane (Fig. 4). Thicker recrystallised grains were

Table 1 Friction stir welding parameters and tool geometry

Travelling speed, mm min^{-1}	Rotational speed, rev min^{-1}	Pin diameter, mm	Shoulder diameter, mm
480	1200	4·2	13

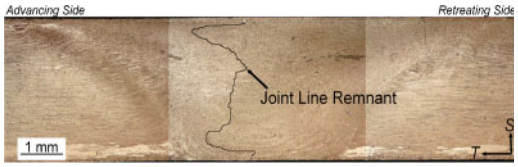

6 Light optical micrograph of weld with JLR: JLR line redrawn artificially to highlight its morphology

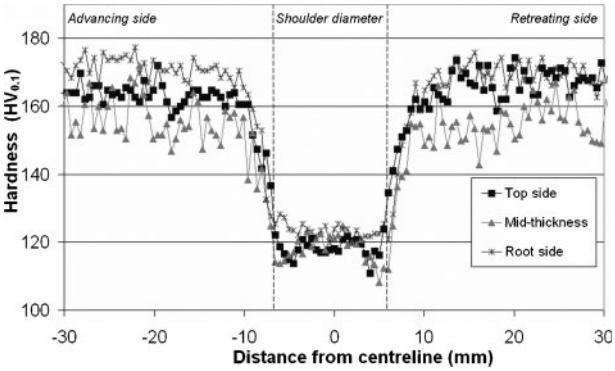

7 Microhardness profiles across the sound weld

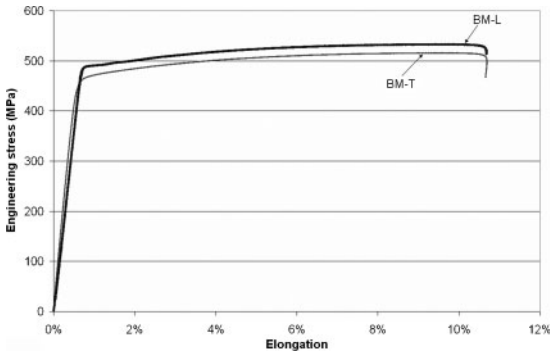

8 Engineering tensile curves for the base material

observed in the T–S and L–S planes close to the surfaces. The observation by optical microscopy of weld microstructure reveals three zones (*see* Fig. 5):

(i) weld nugget (WN) is composed of fine equiaxed grains of typical size between 5 and 10 μm
(ii) thermomechanically affected zone (TMAZ) is composed of highly deformed grains
(iii) heat affected zone (HAZ) has the same grain structure as the base material.

In the sound weld (Fig. 5), no defect, such as JLR, porosity or cracks was observed by optical microscopy at any weld location. In the micrograph of the material welded after natural oxidation, a JLR can be seen (Fig. 6). It consists of a discontinuous zigzag curve of oxide particles through the sheet thickness.

Hardness and tensile properties

Figure 7 shows the hardness profile through the sound weld at three different distances from the weld top (heated by the tool shoulder). It can be seen that the weld zone is softer than the base material. At 10 mm from the centreline, hardness decreases down to a minimum in the WN, the TMAZ and a part of the HAZ (120 HV0.1). The weld zone is softer by about 50 HV0·1 than the base material. This difference is consistent with measurements made on welded T851 Al–Cu–Li alloys.[18,19] Only very limited differences were observed between the top, the middle and the bottom of the weld. A minimum in hardness can be observed in the TMAZ on the retreating side at mid-thickness with a reduction of 10 HV0·1 with respect to the WN. Figure 8 shows a slight anisotropy in tensile properties for the base material. The yield stress and tensile strength of the base material along the T direction are lower by 4 and 3% respectively than those of the base material along the L direction (Table 2). A similar difference between the L and T directions is measured by Steglich *et al.*[3] for tensile tests on a 2198-T8 alloy (thickness 3·1 mm). Cavaliere *et al.*[20] noted a more pronounced anisotropy in tensile properties in a 2198-T8 alloy (thickness 4 mm) with decreases of 20 and 12% in yield stress and the tensile strength respectively along the T direction compared to those along the L direction. Figure 9 shows a tensile curve for the sound weld. Note that the initial gauge length was 25 mm so that the elongation measurement only provides an averaged value over the entire weld. The amount of strain in the softer zones may be substantially higher than that in the base material. Yield stress and tensile strength of welded specimens are 255 and 403 MPa respectively, which means that the yield strength is almost half that of the base material. The work hardening capacity of the welded material is substantially higher than that of the base material. The joint efficiency, which is the ratio between the ultimate strength of the welded joint and that of the base material (along the T direction), is 78%. This value is similar to that obtained by Denquin *et al.*[18] on 2098-T8 FSW assemblies (thickness 3 mm). However, as fracture could have occurred by strain localisation, tensile strength and joint efficiency might also depend on specimen geometry. In the present study, fracture occurred in the weak zone, in the TMAZ on the retreating side.

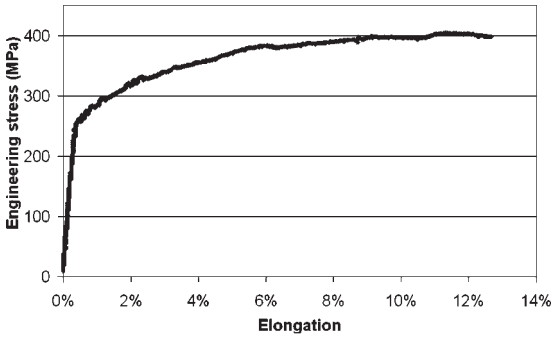

9 Cross-weld engineering tensile curve of sound weld: elongation strongly depends on initial gauge length

Table 2 Tensile tests results

	Yield strength, MPa	Tensile strength, MPa
Base material along L direction	490	530
Base material along T direction	470	515
Sound weld	255	403

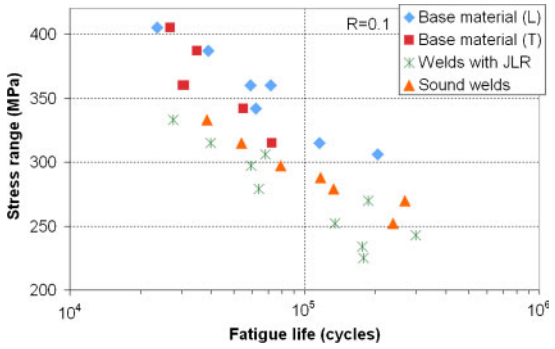

10 S–N curves of base material and welded specimens

Fatigue properties

The fatigue properties of both base material and welded joints are given as S–N curves in Fig. 10. The stress range corresponding to a fatigue lifetime of 100 000 cycles will be considered here, i.e. the targeted lifetime of welded parts for the aimed aircraft application. Its value is about 315 MPa for the base metal; very little difference can be seen between results along both L and T directions. For high stresses, however, fatigue life tends to be lower for specimens tested along the T direction. These results are different from those obtained by Cavaliere *et al.*,[20] which show a difference in fatigue strength at 100 000 cycles between tests along the L and T directions of about 10%, for 2198-T8 (thickness 4 mm) fatigue specimens tested with loading ratio R=0·33. However, the material anisotropy in tensile properties was also more pronounced than that in the present study.

Concerning sound welds, the stress range is about 290 MPa (i.e. a stress reduction of about 10% compared to the base material), whereas for the welded material containing a JLR, the stress range is about 270 MPa, i.e. about 15% lower than the corresponding stress for the base material. The reduction in fatigue lifetime due to the JLR defect is very limited under the current testing conditions. The same reduction (about 10%) was measured by Cavaliere *et al.*[20] when comparing the stress ranges at 300 000 cycles for 2198-T8 base material tested along the T direction and 2198 FSW assemblies (R=0·33). Concerning fatigue crack initiation, failure of sound welds took place in the TMAZ/HAZ for four out of seven specimens and in the WN for the three remaining specimens. For welds containing a JLR, four out of 10 specimens failed in the TMAZ/HAZ and six out of 10 failed in the WN. For three out of the six specimens that failed in the WN, the crack initiation region is close to the JLR. However, the fatigue lifetime

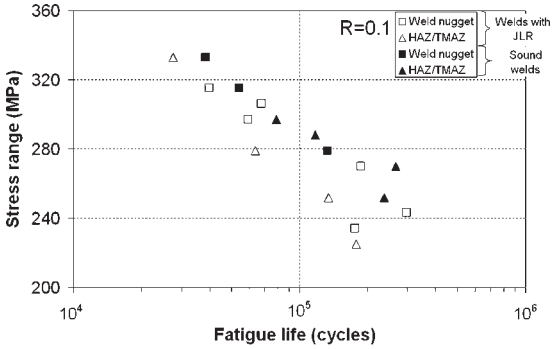

11 S–N curves of sound welds and welds with JLR linked to fatigue crack initiation location

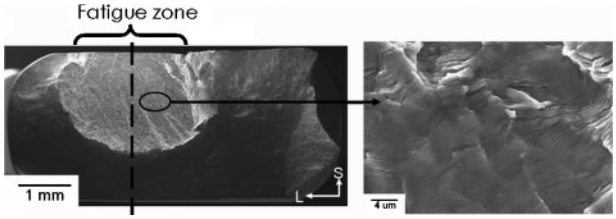

12 Typical SEM images of fracture surface of welded fatigue specimen with JLR: specimen was then cut along dotted line and observed in T–S plane

of these three samples is not reduced compared to the samples that failed in the TMAZ/HAZ or in the WN far from the JLR (Fig. 11). Figure 12 shows a typical SEM image of a failed specimen of the welded joint containing a JLR. The circularly shaped fatigue crack propagation area can clearly be distinguished from the final fracture zone. In order to identify the fatigue crack initiation area with respect to the JLR, the sample was then cut through the fatigue fracture zone (see dotted line), polished and etched. The corresponding light optical micrograph (Fig. 13*a*) showed that the fatigue crack initiated within the WN. In other specimens, the fatigue crack initiated in the TMAZ/HAZ (Fig. 13*b*) or in the WN close to the JLR (Fig. 13*c*). All the fatigue cracks initiated from the specimen surface and half of the fatigue cracks initiated from the specimen corner (despite the grinding) without any difference between base material and welds.

Discussion

The present experimental results show that the reduction in fatigue strength for a lifetime of 100 000 cycles, for the chosen experimental parameters, for the sound welds and welds with JLR compared to the base material is moderate (about 10 and 15% respectively). The effect of the JLR on the fatigue lifetime is very limited under these testing conditions. The fatigue fracture initiation location

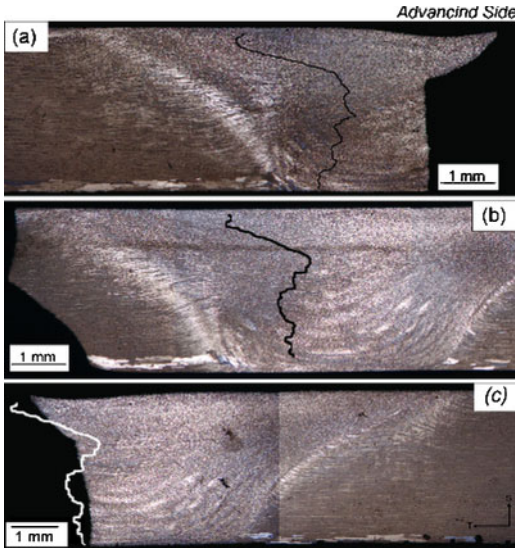

a in WN; *b* in TMAZ/HAZ; *c* next to JLR

13 Light optical micrographs of three representative failed welded fatigue specimens observed in T–S plane for failure location: JLR line has been redrawn for clarity in all three micrographs; advancing side on right

is hardly affected by the presence of the JLR. For the specimens that failed close to the JLR (30%) no reduction in fatigue lifetime could be evidenced in comparison with JLR bearing specimens that failed at other locations. The reduction in tensile properties such as yield strength is much more pronounced between welds and base material (from 470 for the base material to 255 MPa for cross-weld specimens) than the reduction in fatigue strength. This means that for all maximum stress levels chosen for fatigue tests, the welded material deformed plastically, at least during the first quarter of the first cycle, which means that prestrained material is subsequently tested. In the WN, tensile residual stresses along the cross-weld direction have been identified,[4,21] which may be detrimental to the fatigue strength. Owing to plastic deformation induced by the first fatigue cycle, these stresses are however expected to be redistributed and not to affect the present results. For the geometrical stability of the welded structure, this clearly means that the structure elongates plastically during the first quarter of cycle and the geometry of the specimen is changed for the subsequent cycles. This drawback might be overcome by prestraining the entire welded structure before aircraft assembly. For the present testing conditions ($R=0{\cdot}1$), the material is loaded under tension during the entire cycle. If the plastically strained part of the weld hardened through kinematic hardening and if the material was loaded under tension–compression, the fatigue lifetime of the weld might be substantially lower, as the material would undergo macroscopic plastic deformation during each cycle. Owing to the material thickness, 3·1 mm, it would be very difficult to perform tension–compression tests using the current test set-up because of buckling problems. Testing of the material through bending and fully reversed loading ($R=-1$) might be a way to assess this effect experimentally. Owing to the geometry of the weld zones and the inclined orientation of the weakest zone (TMAZ), plastic deformation during the first quarter of the first cycle may lead to compressive residual stresses that may be beneficial for the fatigue lifetime of the weld. Further measurements of the hardening behaviour of the different weld zones in the first quarter of cycle are necessary to better understand the weld behaviour. In this study, the material has not been tested for higher numbers of cycles, at loads where the weld zones do not deform macroscopically by plasticity. In order to further investigate the influence of the JLR on fatigue lifetime of the weld it would be interesting to assess the fatigue behaviour at higher numbers of cycles. This is, however, beyond the scope of both industrial application and of the present study.

Conclusions

In this study, an experimental investigation of the mechanical and fatigue properties of 2198 alloy in T851 condition, friction stir sound welds and friction stir welds with a JLR defect has been carried out leading to the following conclusions:

1. There is a strong influence of FSW on tensile properties since the yield strength and tensile strength of friction stir welds are reduced respectively by 45 and 22% compared to those of the base material.

2. The weld microhardness profile shows a weak zone in which a decrease of 50 HV0·1 is observed compared to the value in the base material.

3. The difference between the fatigue strength at 100 000 cycles ($R=0{\cdot}1$) of sound welds and the base material is less pronounced (only 10%). Welds deform plastically, at least during the first cycle.

4. The effect of the JLR defect on the fatigue properties seems to be low since a reduction by only 15% in fatigue strength at 100 000 cycles is observed compared to the base material. Moreover, only in one-third of cases fatigue crack initiation takes place close to the JLR defect and does even not seem to induce any reduction in fatigue lifetime in these cases.

Acknowledgements

The authors would like to thank the French Federation for Aircraft and Space Research for funding this MASAE project. They acknowledge Anne Denquin (ONERA) for providing welds and for technical discussion. Dominique Schuster (EADS), Michel Suéry (INPG), Séverine Paillard (CEA), Jacques Besson and André Pineau (MINES ParisTech) are thanked for technical discussion.

References

1. A. K. Shukla and W. A. Baeslack: *Scr. Mater.*, 2007, **56**, (6), 513–516.
2. R. W. Fonda, J. F. Bingert and K. J. Colligan: *Scr. Mater.*, 2004, **51**, (3), 243–248.
3. D. Steglich, H. Wafai and W. Brocks: *Int. J. Damage Mech.*, 2010, **19**, 131–152.
4. G. Bussu and P. E. Irving: *Int. J. Fatigue*, 2003, **25**, (1), 77–88.
5. K. V. Jata, K. K. Sankaran and J. J. Ruschau: *Metall. Mater. Trans. A*, 2000, **31A**, (9), 2181–2192.
6. R. John, K. V. Jata and K. Sadananda: *Int. J. Fatigue*, 2003, **25**, (9–11), 939–948.
7. S. Di, X. Yang, G. Luan and B. Jian: *Mater. Sci. Eng. A*, 2006, **A435–A436**, 389–395.
8. Y. S. Sato, H. Takauchi, S. H. C. Park and H. Kokawa: *Mater. Sci. Eng. A*, 2005, **A405**, (1–2), 333–338.
9. H. B. Chen, K. Yan, T. Lin, S. B. Chen, C. Y. Jiang and Y. Zhao: *Mater. Sci. Eng. A*, 2006, **A433**, (1–2), 64–69.
10. Y. Uematsu, K. Tokaji, H. Shibata, Y. Tozaki and T. Ohmune: *Int. J. Fatigue*, 2009, **31**, (10), 1443–1453.
11. T. Vugrin, M. Schmücker and G. Staniek: in 'Friction stir welding and processing III', (ed. K. V. Jata *et al.*), 277–284; 2005, Warrendale, PA, TMS.
12. T. L. Dickerson and J. Przydatek: *Int. J. Fatigue*, 2003, **25**, (12), 1399–1409.
13. C. Z. Zhou, X. Q. Yang and G. H. Luan: *Mater. Sci. Eng. A*, 2006, **A418**, (1–2), 155–160.
14. C. Zhou, X. Yang and G. Luan: *Scr. Mater.*, 2006, **54**, (8), 1515–1520.
15. C. Z. Zhou, X. Q. Yang and G. H. Luan: *J. Mater. Sci.*, 2006, **41**, (10), 2771–2777.
16. G. M. D. Cantin, S. A. David, W. M. Thomas, E. Lara-Curzio and S. S. Babu: *Sci. Technol. Weld. Join.*, 2005, **10**, (3), 268–280.
17. 'Standard practice for conducting force controlled constant amplitude axial fatigue tests of metallic materials', E466-07, ASTM, West Conshohocken, PA, USA, 2007.
18. A. Denquin, D. Allehaux, G. Lapasset and H. Ostersehlte: Proc. 11th Int. Conf. on 'Aluminium alloys', Aachen, Germany, September 2008, DGM, 1939–1944.
19. G. Pouget and A. P. Reynolds: *Int. J. Fatigue*, 2008, **30**, (3), 463–472.
20. P. Cavaliere, A. de Santis, F. Panella and A. Squillace: *Eng. Fail. Anal.*, 2009, **16**, (6), 1856–1865.
21. M. Peel, A. Steuwer, M. Preuss and P. J. Withers: *Acta Mater.*, 2003, **51**, (16), 4791–4801.